SOLAR ARRAY FLIGHT DYNAMIC EXPERIMENT

RICHARD W. SCHOCK

NASA/MARSHALL SPACE FLIGHT CENTER

Presented at

WORKSHOP ON STRUCTURAL DYNAMICS AND CONTROL
INTERACTION OF FLEXIBLE STRUCTURES

MARSHALL SPACE FLIGHT CENTER, ALABAMA

APRIL 22-24, 1986

SOLAR ARRAY FLIGHT DYNAMIC EXPERIMENT

Richard W. Schock

ABSTRACT

The purpose of the Solar Array Flight Dynamic Experiment (SAFDE) is to demonstrate the feasibility of on-orbit measurement and ground processing of large space structures' dynamic characteristics. Test definition or verification provides the dynamic characteristic accuracy required for control systems use. An illumination/measurement system was developed to fly on space shuttle flight STS-41D. The system was designed to dynamically evaluate a large solar array called the Solar Array Flight Experiment (SAFE) that had been scheduled for this flight. The SAFDE system consisted of a set of laser diode illuminators, retroreflective targets, an "intelligent" star tracker receiver and the associated equipment to power, condition, and record the results. In six tests on STS-41D, data was successfully acquired from 18 retroreflector targets and ground processed, post flight, to define the solar array's dynamic characteristic. The flight experiment proved the viability of on-orbit test definition of large space structures dynamic characteristics. Future large space structures controllability should be greatly enhanced by this capability.

SOLAR ARRAY FLIGHT DYNAMIC EXPERIMENT

Richard W. Schock
NASA Marshall Space Flight Center
Huntsville, Alabama

INTRODUCTION

In September of 1984, NASA flight tested the Solar Array Flight Dynamic Experiment (SAFDE) on STS-41D. The purpose of this experiment was to demonstrate the feasibility of on-orbit measurement and ground processing of large space structure dynamic characteristics. The dynamic characteristics are structural natural frequencies, mode shapes, and damping. Accurate definition of these characteristics are necessary for large space structures with active control systems to prevent structure/control system interaction. In past vehicles and on-orbit structures, the structural natural frequencies were significantly higher than the control system frequencies. However, with large space structures, the structural natural frequencies are so low that the control natural frequency will either be very close to the first natural structural frequency or nested between a pair of the lower natural structural frequencies. This problem, coupled with the dense rate of structural frequencies, requires a very accurate definition of the structural characteristics. Unfortunately, large space structures are designed for zero-g use and cannot be adequately tested in one-g environments. On-orbit test, therefore, is the remaining alternative to verify analysis results or define correct values where analysis results are inacurate.

To investigate the feasibility of on-orbit large space structure dynamic testing, a dynamic augmentation experiment (SAFDE) was added to an existing flight test called the Solar Array Flight Experiment, SAFE (Fig. 1). The SAFE was indeed an unprecedented opportunity since it flew early and has the characteristics of a large space structure. These characteristics are shown in Table 1.

Table 1

SOLAR ARRAY STRUCTURAL CHARACTERISTICS

o Array Wt	
o Blanket	225 kg
o Mast	132 kg
o Container	40 kg
o Cover Assembly	40 kg
o Natural Frequencies	0.033-0.4 Hz
o Array Length	3100 cm
o Array Width	400 cm

As noted, the array has extremely large area to weight ratios and low natural frequencies (0.03 Hz). In atmospheric conditions, air damping dominates over the structural damping, and the array cannot be dynamically tested in one-g. A dynamic augmentation to the SAFE was authorized, and an experiment was developed and integrated into the shuttle orbiter.

MEASUREMENT SYSTEM DEVELOPMENT

In order to measure the solar array dynamic motion, an illumination, remote sensing and recording system had to be developed. The general requirements for the measurement system are to illuminate and track a set of 23 retroreflective targets. The displacement of the targets are measured, converted to engineering units, multiplexed, and stored on a digital tape recorder. Post flight, the data is ground processed to obtain dynamic characteristics of the array.

The specific measurement system requirements are as follows:

1. Simultaneously track 23 retroreflective targets on the solar array.
2. Accuracy requirement, 19 arc seconds.
3. Update rate, 2 Hz.
4. Total target displacement, ±45 cm.
5. Target speed, 6.28 cm/sec.
6. Field of view, 19 x 19 degrees.
7. Survive launch environments.
8. Operate in on-orbit environments, with no active cooling.

The measurement system to accomplish these objectives was developed by the Marshall Space Flight Center and is shown in flow diagram form on Fig. 2. The system consists of the following:

1. Retroreflector field tracker (RFT) containing-
    a. Laser diode illuminators.
    b. Solid state sensor.
    c. Microprocessor.
2. Twenty-three retroreflector targets mounted on the array.
3. Multiplexer (PCM).
4. Digital tape recorder (TR).
5. Power control and distribution assembly (PCDA).

As shown on Fig. 2, the PCDA receives and distributes power, commands and talk back, and experiment health information. The RFT was the major development item, and was designed and built by Ball Aerospace Systems Division[1]. It consists of two hardware items, the illuminator/sensor assembly and the microprocessor. The illuminator sensor assembly is mounted 1.9 meters (75 in.) from the base of the array blanket on the mast side of the blanket. Basically, it has a circular cross section 24 cm (9.45 in.) in diameter by 56.4 cm (22.2 in.) in length, and weighs 7.5 kg (16.8 lbs). The microcomputer is a part of the main electronics box (MEB) which sets on the mission peculiar support structure (MPSS) remote from the sensor. This package is 24.6 x 21.6 x 39.4 cm (9.7 x 8.5 x 15.5 in.) in size and weighs 16.1 kg (35.4 lbs.)

During operations the RFT illuminates the solar array with five laser diode sources which are independently projected onto the solar array. The lasers are 30-milliwatt diodes operating at 820 nanometers. The source illumination is lensed so that the maximum intensity is at the top of the array. The illumination is returned by retroreflector targets to the illumination source. The targets are of varying sizes, from 14 mm (0.55 in.) to 42 mm (1.6 in.), and arranged proportionately to the distance from the sensor. The combination of illumination intensity and reflector size provided a near uniform image intensity to the sensor focal plane. The retroreflector targets were small aluminum standoffs, attached over a solar array hinge. These were designed to stand off perpendicular to the solar array blanket when the blanket was deployed and fold neatly into the blanket folds when the blanket was stowed. Additional rigid targets were attached to the mast, topcover, and tip fitting. The retroreflective surface was a high gain commercially produced retroreflective tape. The retroreflectors are shown in Fig. 3.

The reflector images are focused on a solid state, charge injection device (CID) detector. The detector consists of a 256 x 256 pixel array, each 0.02 millimeters square in an active area of 5 x 5 mm. The detector interrogation is controlled by the microprocessor. The tracking rate is defined by the track algorithm and the target velocity. The track algorithm requires the target motion of the detector to be limited to one pixel per update period. The maximum required velocity of the array is 6.28 cm/sec at the closest target (790 cm or 311 in.). This rate becomes 5.1 pixels/sec. A track rate of 6 Hz was selected to meet this requirement even though the output rate is 2 Hz. The accuracy requirement of 19 arc seconds translates into approximately 1/4000 of the field of view (FOV). This necessitates interpolation to approximately 6.4 percent of a pixel. This interpolation accuracy was met using a star tracker interpolation algorithm.

When the RFT is powered, after an internal self test and initialization, it begins a search and acquisition routine. In each data cycle, the laser illuminator is pulsed to "freeze" the target motion, and the return signal is integrated on the detectors. A 12 x 12 pixel search block is read out and compared to a threshold to determine if a target is present. If one is found, its position is compared to the stored map for identification, a track loop locks onto its position, and it is added to the list of targets being tracked. This function takes approximately 80 seconds.

After the initial search, the same sequence is continually performed, except that the sensor also tracks the target positions. The continued search performs a scavenger function to find targets that may have been missed initially or lost after acquisition. Each target is read out twice per track sequence, once after the laser diodes have been strobed, and once after the CID is injected and the background is accumulated for a time equal to the laser pulse. The difference resulting from the double read is generated on a per pixel basis, and the background noise is thus eliminated.

The software system must provide for simultaneous tracking and acquisition, since tracking of early acquired targets must continue while later targets are acquired. Once all targets are acquired, if a target is lost, the acquisition routine reverts from its normal fixed pattern routine, to a search routine initiated at the last known position of the target. This allows reacquisition of a "lost" target to occur in a maximum of 324 msec.

The numbering of each target was a challenging problem. The array was to be at either 100 percent or 70 percent of full deployment. At 100 percent, 23 targets were visible; at 70 percent, 18 targets were visible. The microprocessor was, therefore, given an expected map of both arrays, and the acquisition system had to be manually "cued" prior to flight test to tell it which set of algorithms to use. If, because of some unforeseen problem, the targets did not appear in their prescribed "areas," then target numbering was done on a first-come-first-served basis until all 18 or 23 assignments were filled. The prescribed geometric algorithms to change angular deviations to engineering displacement would obviously be incorrect. However, the sensor output also included the raw angular deviations which, post test, would allow data evaluators to reconstruct the locations and displacements. Since the solar array "warped" significantly during test, this is, in fact, what happened and will be discussed later in data evaluation.

The RFT successfully completed full flight performance and qualification tests as a unit at the contractor and later as a complete system at Marshall Space Flight Center. Actual tracking accuracy of 10 arc seconds proved better than specification of 19 arc seconds.

EXPERIMENT INTEGRATION AND MISSION OPERATIONS

The SAFDE was physically integrated with the remainder of the OAST-1 mission as shown in Fig. 4. The illuminator/sensor was positioned on a stiff support system 1.9 m (75 in.) in the x-direction from the array blanket. The optic axis is tilted 14.8 degrees from the z-axis to optimize the field of view. This provides a target pattern which is very wide at the base and narrow at the top. The 14.8 degrees was chosen to minimize deflection errors, yet ensure that under maximum deflection conditions, no target was obstructed by solar array structure. Accurate alignment accuracies obtained were ±5 arc minutes.

The SAFDE was a part of a multimission payload called OAST-1. OAST-1 consisted of the Solar Array Flight Experiment, the SAFDE, a photogrammetric experiment with similar objectives but different techniques[2] from

the SAFDE, and a solar cell calibration experiment. Although, the SAFDE and the photogrammetric experiment both measured solar array dynamic deflections, the SAFDE could only operate during orbital night, and the photogrammetric experiment required good sunlight illumination. Adequate operational time was available to do one each on an orbit, so the dynamic tests were run back-to-back. To ensure uniformity of initial conditions, the SAFDE experiment required 10 minutes of "orbiter quiescence" prior to solar array excitation. The SAFDE could not operate with the bright moon in the field of view. Since the orbiter was under attitude control prior to the "quiescent period," and the last Vernier control reaction system (VCRS) pulse was a random process, and since relatively high rates of drift occurred with the solar array extended, the exclusion of the moon from the field of view could not be guaranteed. The severity of the problem changed with the time of the month the flight was to occur. At the final mission time, the moon relationship was such that it set shortly after orbital midnight, which allowed sufficient time to test prior to sunrise with no "moonshine" problem. This operational constraint can be "cured" by more powerful illuminators. Typically, an operational sequence would be the following scenario.

1. Initiate "quiescence" 10 minutes prior to moonset.

2. Perform illumination/sensing system setup and checking functions.

3. At moonset, turn illumination/sensor system on.

4. Excite array with orbiter VRCS.

5. Take data for 12 minutes.

6. Turn off sensor system and terminate test.

Due to safety concerns about exciting the 100-percent-deployed array on the dark side, only 70-percent-deployment tests were performed on the SAFDE. Six excitations were applied to the solar array for the SAFDE test. They included out-of-plane, in-plane, and multimodal tests. The out-of-plane test was a pitch maneuver of the orbiter. The in-plane test was an attempt at a roll maneuver. The orbiter could not perform a pure roll maneuver with the Vernier rate control system; therefore, an incremental maneuver was used. The multimodal maneuver was basically pitching the diagonal corners of the orbiter as to obtain as many modal responses as possible. A further orbiter mission requirement was that the residual rates, after the excitation, be minimized. Therefore, if a positive rotation was placed on the orbiter, it would have to be countered by an equal and opposite impulse to bring the rotation to zero. This requirement resulted in impulse couplets being applied as shown in Fig. 5. The integration and flight operations proved not only adequate but conservative, since additional tests were able to be performed.

FLIGHT RESULTS

Data was obtained on all targets, on all tests, even though some targets were outside of the sensor design range due to the array's darkside

curvature. The array excitations and data take started near orbital midnight and continued for 12 minutes. The blanket curvature shown on Fig. 7 was measured just prior to array excitation or near orbital midnight. The maximum measured curvature was 40 cm in depth.

The 18 targets for the six 70-percent tests each provided x- and y-displacement data for a total or 36 data samples per test. All 36 data samples were simultaneously evaluated by two different response analysis techniques. Both techniques utilize a time-domain curve fit of the data to obtain the modal damping information, and a fast Fourier transform technique to obtain modal amplitude and phase relationships.

The solar array was dynamically evaluated both at orbital midnight by the Marshall Space Flight Center (SAFDE) and at high noon by a Langley Research Center Photogrammetric Experiment[2]. An unexpected curvature formed on the dark side. The result was that the high noon test evaluation closely matched the pretest analytical model, whereas, the SAFDE experiment tested a different structural configuration and did not match pretest analyses. Subsequent post test analyses, using a model which had been modified to account for the previously described mast twist and blanket curvature, improved the analysis/test match but still retained differences.

The structural dynamic natural frequencies and mode shapes, both analytical and measured, are compared in Figs. 8 through 12 and in Table 2.

Table 2

SOLAR ARRAY DYNAMIC CHARACTERISTICS

Analytical Frequency Hz	Mode Shape	Test Frequency	Damping (%)
0.064	Out-of-Plane Bending	0.059 - 0.072	2 - 8
0.067	In-Plane Bending	Not Identified	
0.115	1st Torsion	0.089 - 0.092	1 - 2
0.179	2nd Out-of-Plane Bending	0.121	2 - 4
0.213	2nd Torsion	0.172	2

Neither the photogrammetric nor the SAFDE experiment were able to extract the analytical second mode. This mode is a lateral response, and significant effort was expended to excite it with an in-plane and multimodal test. Mode shapes tended to match well, but natural frequencies not only differed but changed with different test excitations and during decay from each individual excitation. This phenomenom is characteristic of nonlinear structures. The nonlinearity of the structure is illustrated in Figs. 13 and 14. Fig. 13 is a plot of the first mode (out-of-plane deflection) natural frequency versus tip displacement for DAE test No. 1. This test is illustrated because it obtained the maximum tip response of

all tests, therefore providing the largest range of frequency and damping change. The damping change for the same mode, same test is illustrated in Fig. 14. From a tip displacement of 11 cm single amplitude (SA) to 2 cm SA, the damping factor averages about 0.08. Less than 2 cm SA, the factor averages approximately 0.02.

CONCLUSIONS

1. The SAFDE experiment successfully measured the SAFE solar array dynamic response, even under out-of-design conditions.

2. Four of the first five solar array modal characteristics were successfully test determined.

The Solar Array Flight Dynamic Experiment also illustrated a number of points significant to control/structure interaction of large space structures. The solar array was more than just an advance solar array; it was, in fact, representative of a generic class of future large space structures (LSS). The type of construction, strength to weight ratios, natural frequencies, and, most importantly, the inability to adequately dynamic test on the ground are all synonymous with future LSS. Like the LSS, the solar array had very low natural frequencies (0.035 Hz, first mode) and densely spaced modes, greater than 33 modes per Hz. In order to maintain control authority of an LSS with similar characteristics, the control frequency would probably have to be nested among the structural natural frequencies. With the characteristic modal density of LSS, very little frequency "window" would be available to insert the control frequency. This, in turn, would require a highly accurate knowledge of the structural frequencies to avoid control/structure interaction. That accuracy is normally obtained by test verification of the math model, which in the case of large space structures, must be done on-orbit. As previously noted, an unexpected curvature formed on the dark side. The SAFDE experiment, therefore, tested a different configuration than was analyzed pretest and did not match pretest analyses. Model update was required for correlation and verification. Although normal care was taken in design to prepare the solar array for on-orbit use, this anomaly did occur. As such, it may well be representative of "surprises" which occur with any pioneering venture like LSS. With a combination of probable forthcoming surprises, a requirement for highly accurate structural dynamic characteristics, and an inability to ground test to resolve anomalies, on-orbit dynamic tests appear to be a mandatory LSS requirement. This requirement is further supported by the nonlinear behavior illustrated in the preceeding report. The control implication of the nonlinearity is that the already narrow frequency window in which to place a control frequency is further narrowed if the structural frequencies are a function of amplitude. One very favorable indication from the experiment was that the damping of the structure was significantly higher than previous launch or space vehicle experience. And finally, the SAFDE program did demonstrate and confirm the viability of on-orbit test definition of LSS dynamic characteristics.

ACKNOWLEDGEMENTS

The author wishes to thank Mr. Frank Wargocki and Mr. A. Ray of Ball Aerospace Systems Division who were responsible for the contribution on the retroreflector field tracker section.

REFERENCES

1. F. Wargocki, A. Ray, and G. Hall, "Retroreflector Field Tracker (State-of-the-Art Imaging Arrays and Their Application)," Keith N. Prettyjohns, Editor, Proc. SPIE 501, 1984, p. 283.

2. L. Brumfield, R. Pappa, J. Miller, and R. Adams, "Orbital Dynamics of the OAST-1 Solar Array Using Video Measurements," AIAA paper, 85-0758-CP, 1985.

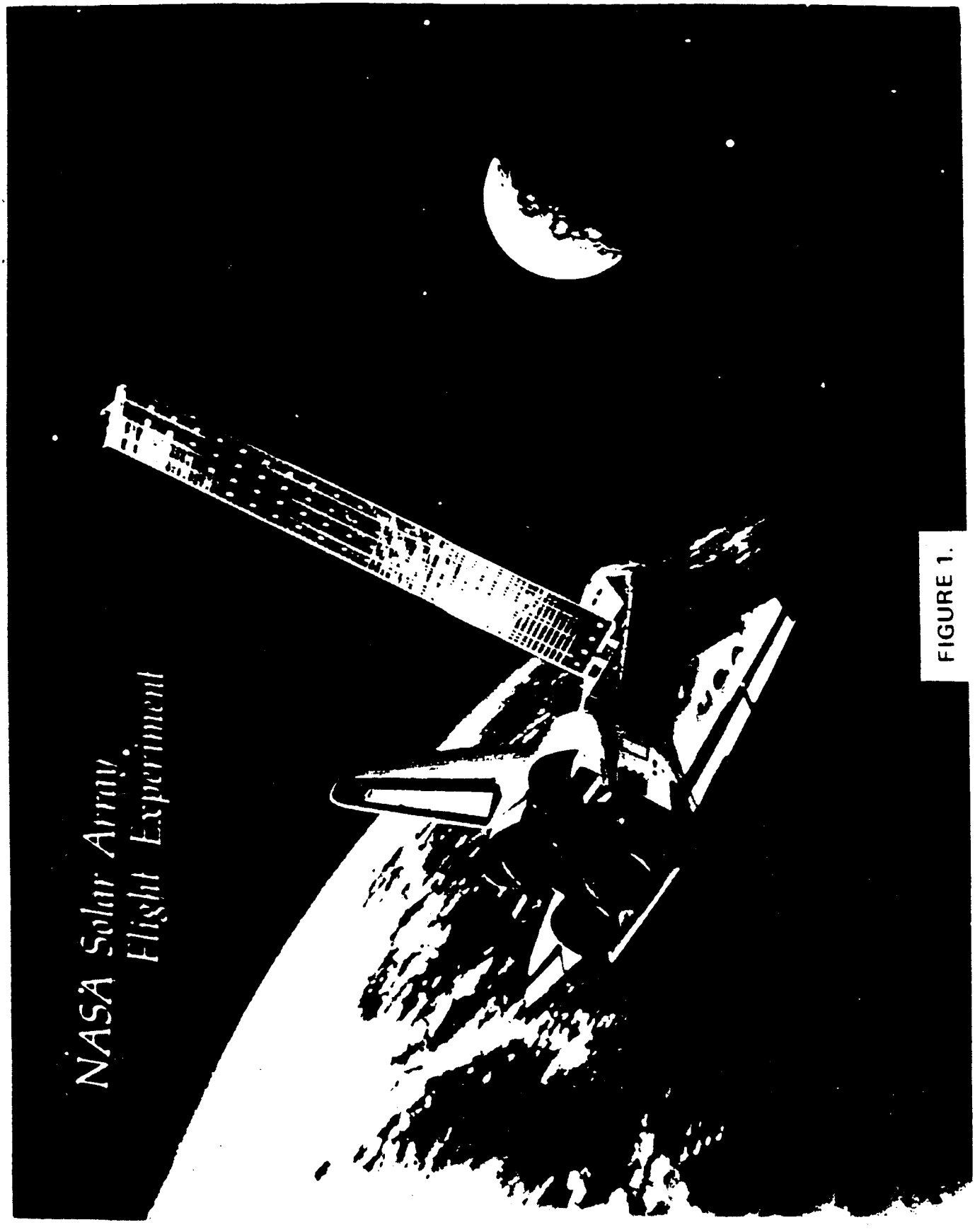

FIGURE 1.

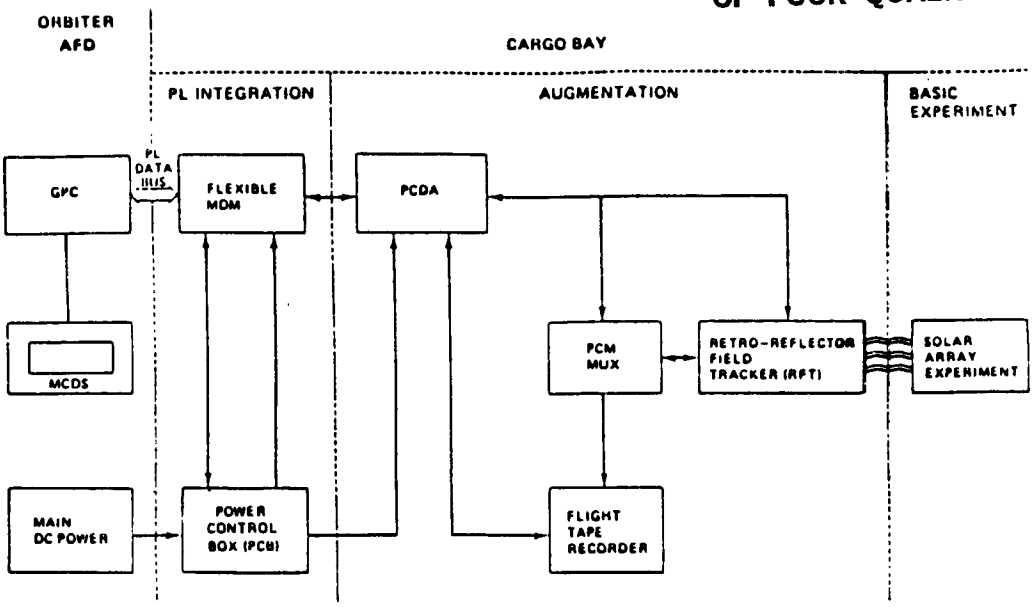

FIGURE 2. SAFDE FUNCTION FLOW

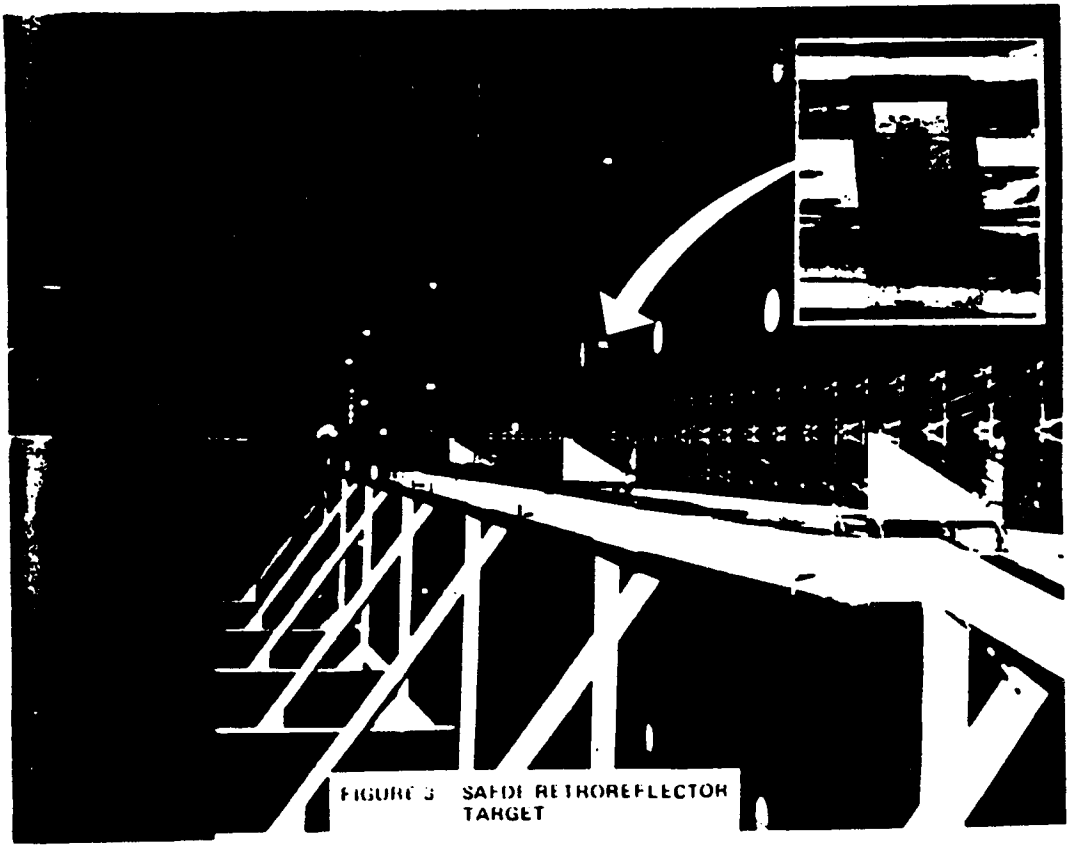

FIGURE 3 SAFDE RETROREFLECTOR TARGET

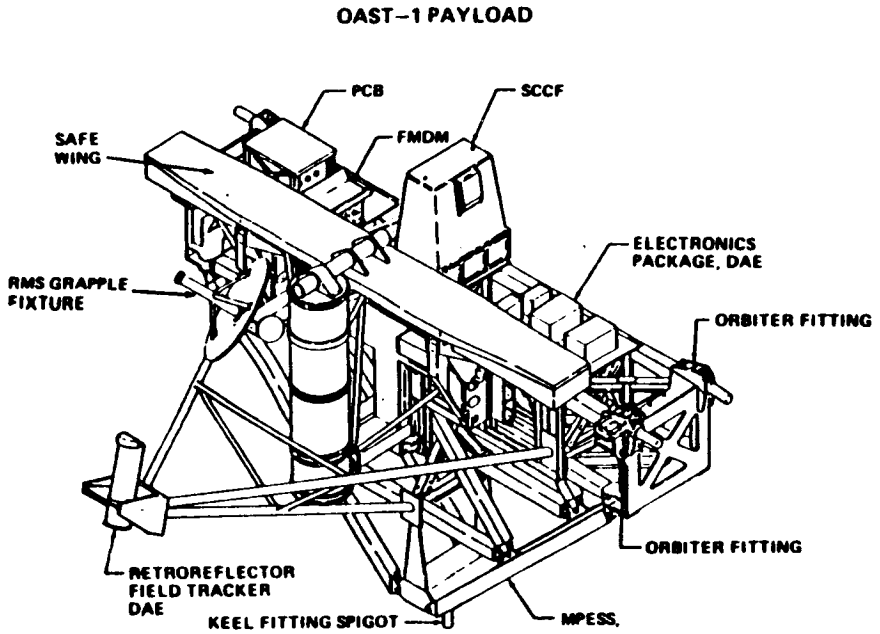

FIGURE 4 OAST-1 SAFE/DAE FLIGHT CONFIGURATION

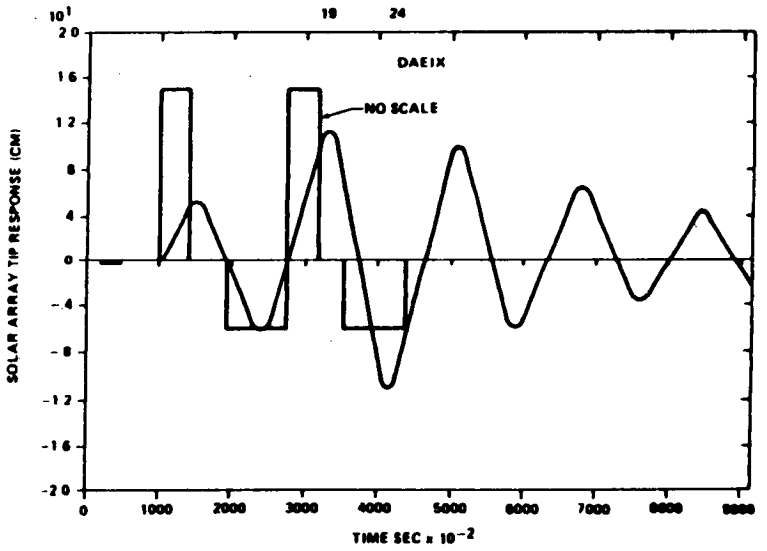

FIGURE 5. 1ST SAFDE ORBITER IMPULSE INPUT AND SOLAR ARRAY TIP RESPONSE

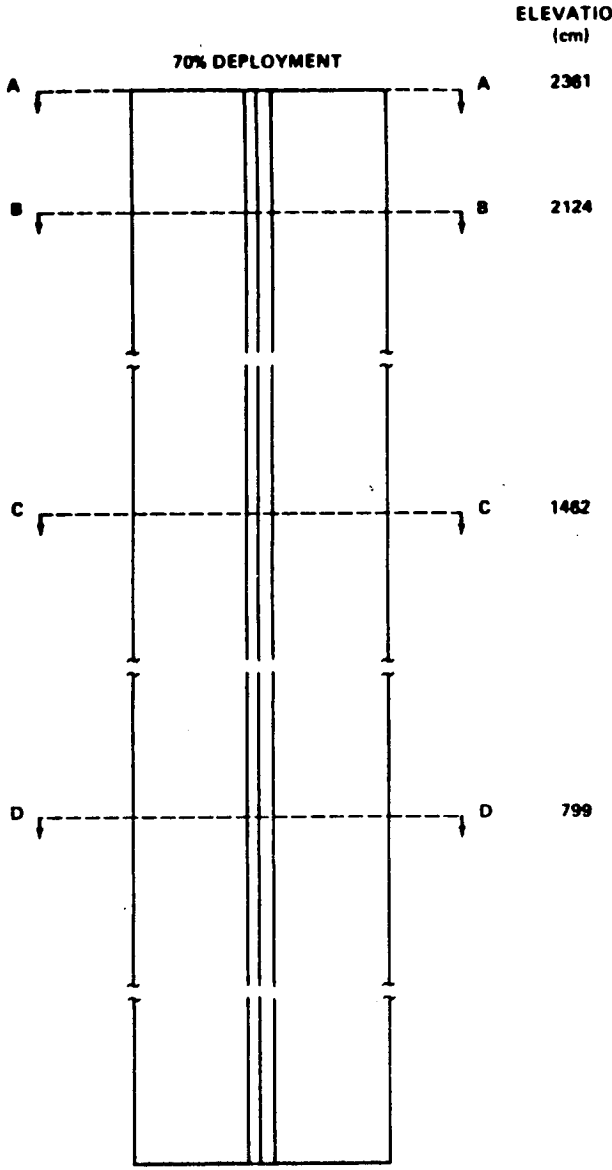

FIGURE 6. WING CROSS SECTIONAL VIEW Y–Z PLANE

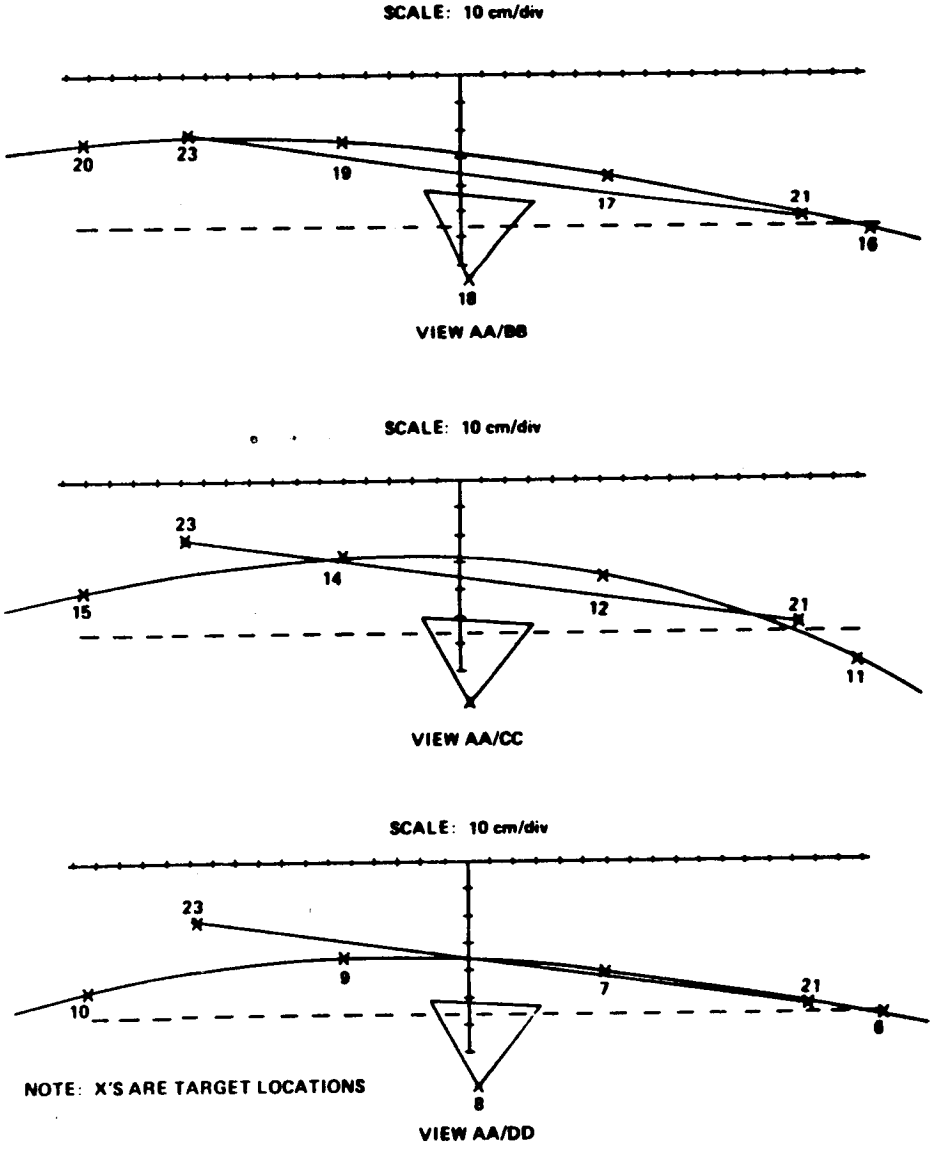

FIGURE 7. BLANKET CURVATURE FIRST SAFDE TEST

ORIGINAL PAGE IS
OF POOR QUALITY

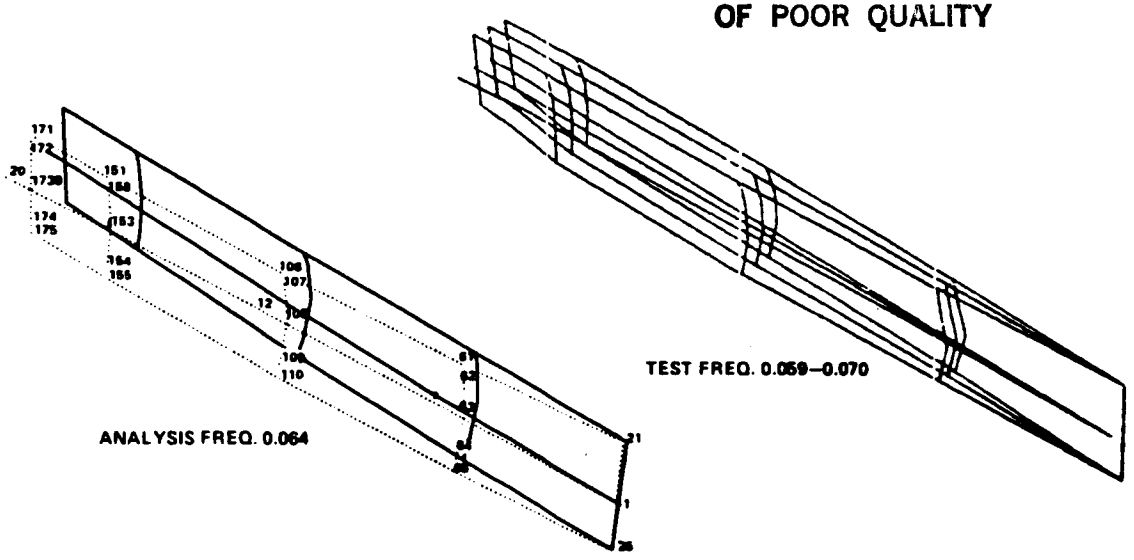

1ST MODE OUT OF PLANE BENDING

FIGURE 8. SOLAR ARRAY DYNAMICS
ANALYSIS/TEST COMPARISON

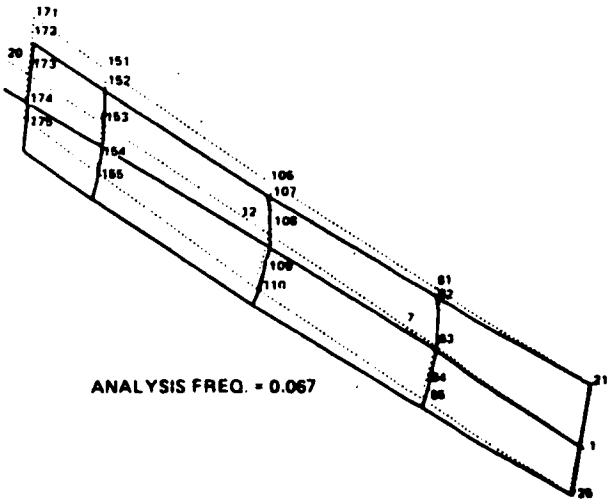

NO
2ND MODE
IDENTIFIED
IN TEST

2ND MODE LATERAL BENDING

FIGURE 9. SOLAR ARRAY DYNAMICS
ANALYSIS/TEST COMPARISON

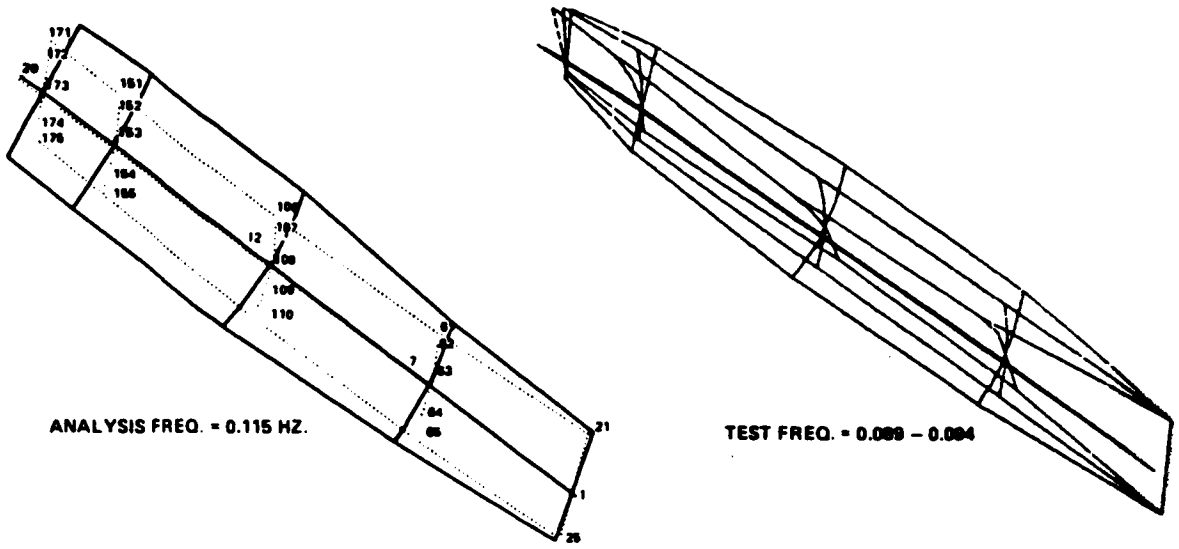

3RD MODE 1ST TORSION

FIGURE 10. SOLAR ARRAY DYNAMICS
ANALYSIS/TEST COMPARISON

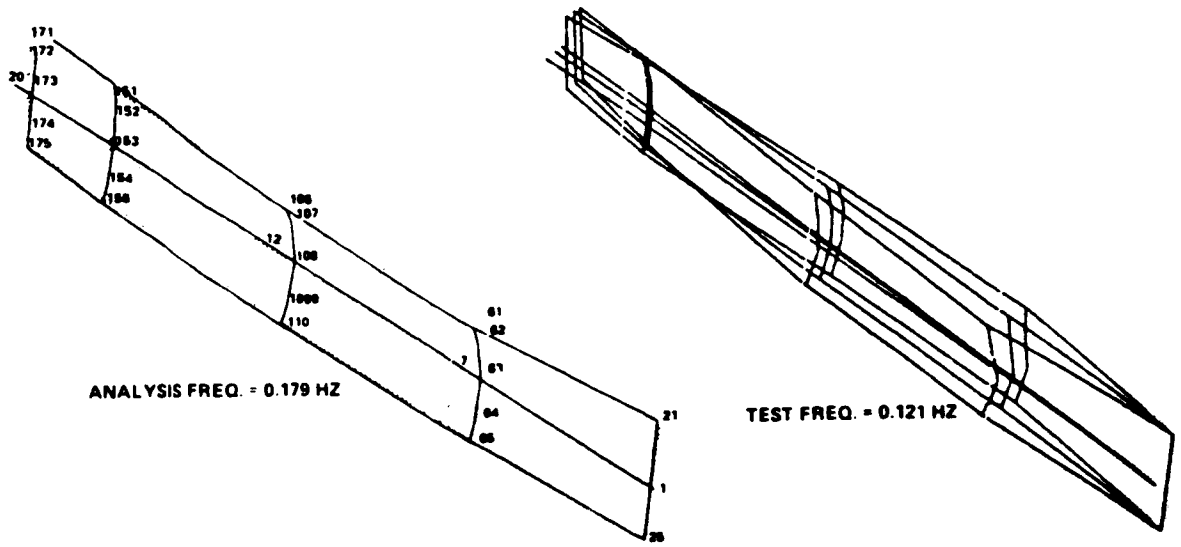

4TH MODE 2ND OUT OF PLANE BENDING

FIGURE 11. SOLAR ARRAY DYNAMICS
ANALYSIS/TEST COMPARISON

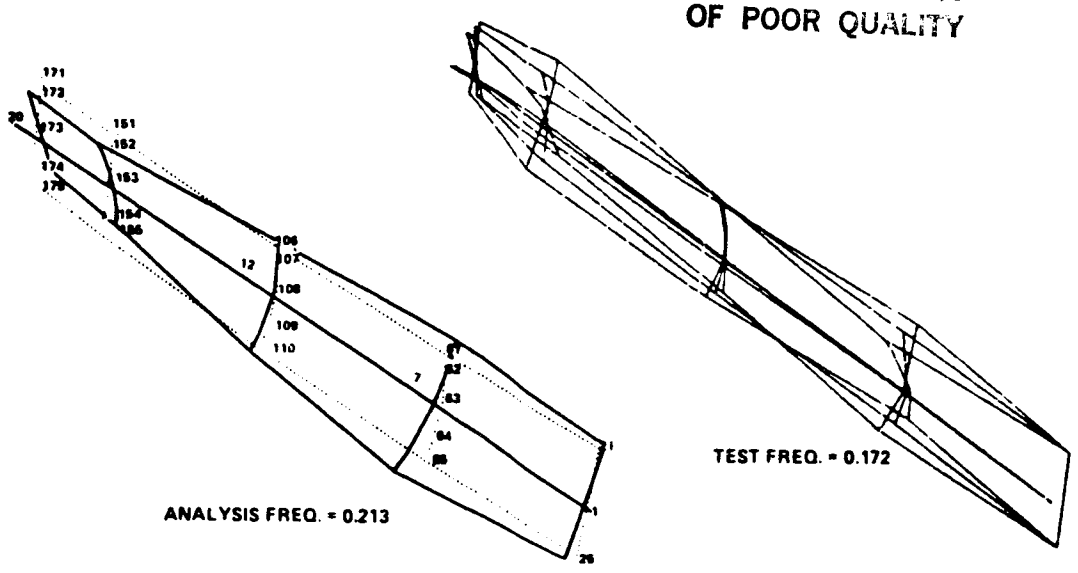

5TH MODE 2ND TORSION

FIGURE 12. SOLAR ARRAY DYNAMICS ANALYSIS/TEST COMPARISON

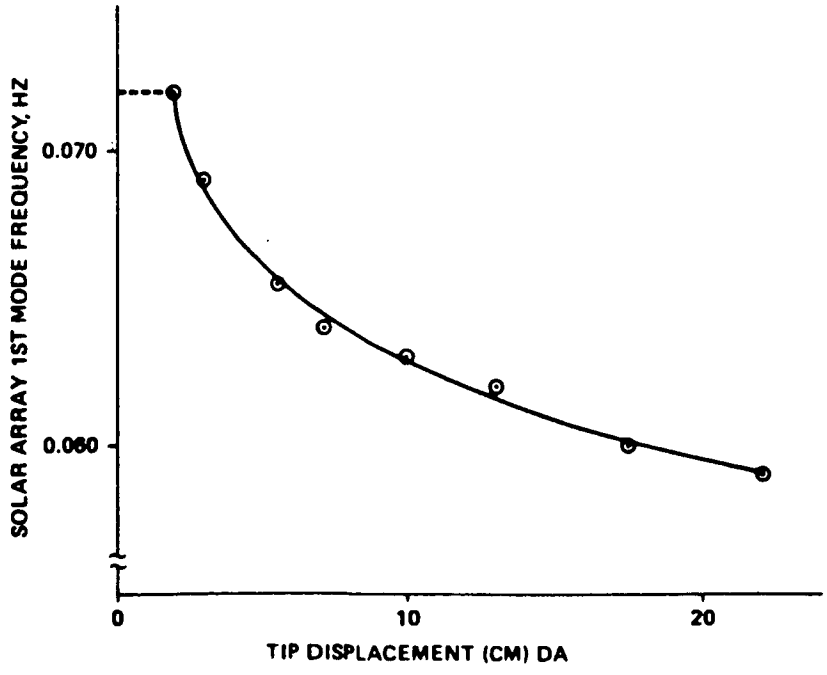

FIGURE 13 1ST MODE NATURAL FREQUENCY VRS TIP RESPONSE DISPLACEMENT

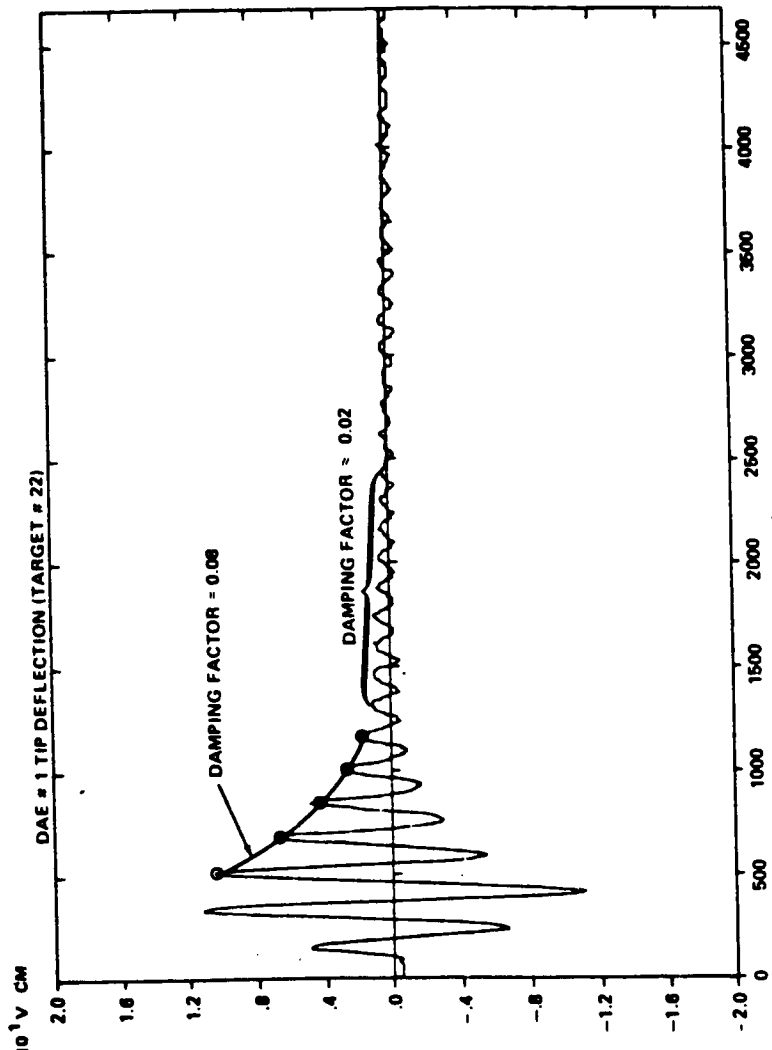

FIGURE 14 SOLAR ARRAY TIP DISPLACEMENT VRS TIME